doi:10.1093/brain/awp028 Brain 2009: 132; 999–1012 | 999

BRAIN
A JOURNAL OF NEUROLOGY

Cortical and subcortical networks in human secondarily generalized tonic–clonic seizures

H. Blumenfeld,[1,2,3] G. I. Varghese,[1] M. J. Purcaro,[1] J. E. Motelow,[1] M. Enev,[1] K. A. McNally,[1] A. R. Levin,[1] L. J. Hirsch,[4] R. Tikofsky,[5] I. G. Zubal,[6] A. L. Paige[7] and S. S. Spencer[1,3]

1 Department of Neurology, Yale University School of Medicine, New Haven, CT 06520, USA
2 Department of Neurobiology, Yale University School of Medicine, New Haven, CT 06520, USA
3 Department of Neurosurgery, Yale University School of Medicine, New Haven, CT 06520, USA
4 Department of Neurology, Columbia University College of Physicians & Surgeons, NY, USA
5 Department of Nuclear Medicine, Columbia University College of Physicians & Surgeons, NY, USA
6 Department of Nuclear Medicine, Yale University School of Medicine, New Haven, Connecticut, USA
7 Department of Neurology, University of Alabama School of Medicine, Birmingham, Alabama, USA

Correspondence to: Hal Blumenfeld, MD, PhD,
Departments of Neurology,
Neurobiology, Neurosurgery, Nuclear Medicine,
Yale University School of Medicine,
333 Cedar Street, New Haven,
CT 06520-8018, USA
E-mail: hal.blumenfeld@yale.edu

Generalized tonic–clonic seizures are among the most dramatic physiological events in the nervous system. The brain regions involved during partial seizures with secondary generalization have not been thoroughly investigated in humans. We used single photon emission computed tomography (SPECT) to image cerebral blood flow (CBF) changes in 59 secondarily generalized seizures from 53 patients. Images were analysed using statistical parametric mapping to detect cortical and subcortical regions most commonly affected in three different time periods: (i) during the partial seizure phase prior to generalization; (ii) during the generalization period; and (iii) post-ictally. We found that in the pre-generalization period, there were focal CBF increases in the temporal lobe on group analysis, reflecting the most common region of partial seizure onset. During generalization, individual patients had focal CBF increases in variable regions of the cerebral cortex. Group analysis during generalization revealed that the most consistent increase occurred in the superior medial cerebellum, thalamus and basal ganglia. Post-ictally, there was a marked progressive CBF increase in the cerebellum which spread to involve the bilateral lateral cerebellar hemispheres, as well as CBF increases in the midbrain and basal ganglia. CBF decreases were seen in the fronto-parietal association cortex, precuneus and cingulate gyrus during and following seizures, similar to the 'default mode' regions reported previously to show decreased activity in seizures and in normal behavioural tasks. Analysis of patient behaviour during and following seizures showed impaired consciousness at the time of SPECT tracer injections. Correlation analysis across patients demonstrated that cerebellar CBF increases were related to increases in the upper brainstem and thalamus, and to decreases in the fronto-parietal association cortex. These results reveal a network of cortical and subcortical structures that are most consistently involved in secondarily generalized tonic–clonic seizures. Abnormal increased activity in subcortical structures (cerebellum, basal ganglia, brainstem and thalamus), along with decreased activity in the association cortex may be crucial for motor manifestations and for impaired consciousness in tonic–clonic seizures. Understanding the networks involved in generalized tonic–clonic seizures can provide insights into mechanisms of behavioural changes, and may elucidate targets for improved therapies.

Received August 28, 2008. Revised December 23, 2008. Accepted January 22, 2009

Keywords: default mode; cerebellum; thalamus; SPECT; epilepsy

Abbreviations: CBF = cerebral blood flow; EEG = electroencephalography; PET = positron emission tomography; SPECT = Single photon emission computed tomographyl; SPM = statistical parametric mapping

Introduction

The most dangerous type of seizure is the generalized tonic–clonic seizure, also known as the grand mal. These frightening events have been described throughout human written history, and give rise to much of the stigmatization and negative consequences of epilepsy. Generalized tonic–clonic seizures can cause injury or death through accidents and falls, and the seizures themselves can produce vertebral fractures, cardiac arrhythmias and when severe or prolonged, rhabdomyolysis, brain damage and death (Drazkowski, 2007; Nei and Bagla, 2007; de Boer *et al*., 2008; Jehi and Najm, 2008). Because of the dramatic motor manifestations of generalized tonic–clonic seizures, they are more difficult to investigate than other seizure types, and few studies have been done in humans to identify the cortical and subcortical networks involved. Emerging evidence suggests that 'generalized' seizures are not truly generalized, but rather affect specific brain regions most intensely, while others are relatively spared (Meeren *et al*., 2002; Blumenfeld *et al*., 2003*b*, Holmes *et al*., 2004; Blumenfeld, 2005*a*; Schindler *et al*., 2007). Identification of the specific cortical and subcortical regions involved in generalized tonic–clonic seizures will be crucial to reach a better understanding of the mechanisms for seizure generation and behavioural impairments, and may also help identify targets for improved prevention or treatment of this seizure type.

Generalized tonic–clonic seizures can occur in primary generalized epilepsy, or can arise from partial seizures with secondary generalization. Over 70% of patients with partial epilepsy occasionally experience secondary generalization (Forsgren *et al*., 1996). After a period of focal features, onset of generalization is usually marked by tonic head or eye deviation, vocalization and asymmetrical tonic contraction of the face (Theodore *et al*., 1994; Jobst *et al*., 2001). This is often followed by irregular clonic jerking evolving into rigid tonic extension of the extremities, which merges into vibratory movements and finally rhythmic clonic jerks. After the seizure ends, in the post-ictal period, patients usually lie still with flaccid muscle tone and deep breathing for a variable period of time before resuming spontaneous movements with some degree of disorientation and confusion. During generalized tonic–clonic seizures, and in the early post-ictal period nearly all patients are deeply unconscious, meaning that they are unresponsive to external stimuli and have no recall of events, with rare exception (Bell *et al*., 1997).

Investigation of generalized tonic–clonic seizures has been limited in both humans and in animal models due to the challenges of performing electrophysiology and imaging studies in the face of generalized convulsions. Animal studies using metabolic labeling methods and post-mortem histology (Handforth and Ackermann, 1995; Handforth and Treiman, 1995; McCown *et al*., 1995), or functional neuroimaging in conjunction with neuromuscular blockade and artificial ventilation (Nersesyan *et al*., 2004; Brevard *et al*., 2006; Schridde *et al*., 2008) have revealed bilateral increases in cortical and subcortical activity in widespread networks. Human investigations of generalized tonic–clonic seizures have been more limited. Early human neuroimaging studies using positron emission tomography (PET) suggested that the whole brain may be involved in generalized tonic–clonic seizures (Engel *et al*., 1982). A recent study with intracranial electroencephalography (EEG) demonstrated that secondarily generalized tonic–clonic seizures often spare some cortical brain regions (Schindler *et al*., 2007). In addition, neuroimaging during induction of generalized tonic–clonic seizures under neuromuscular blockade for treatment of depression has demonstrated that focal cortical and subcortical structures are involved, including regions of the fronto-parietal association cortex, thalamus, brainstem and cerebellum, while other areas are relatively spared (Blumenfeld *et al*., 2003*a*, 2003*b*; Enev *et al*., 2007; Takano *et al*., 2007).

Although these prior studies are informative, the detailed cortical and subcortical networks involved in human spontaneous tonic–clonic seizures have not been thoroughly investigated. Intracranial EEG studies have excellent temporal resolution, but limited spatial sampling especially with regard to subcortical structures. Seizures induced by electrical stimulation in depressed patients under anaesthesia may differ from spontaneous seizures in patients with epilepsy. Animal models enable well-controlled and invasive studies, but do not fully replicate human seizures. Neuroimaging with functional MRI or PET during human tonic–clonic seizures is not practical, since images would need to be obtained during seizures, causing safety concerns, movement artifact and unacceptable waiting time in the scanner. Single photon emission computed tomography (SPECT) has the unique advantage that injection of the radiopharmaceutical is done during the seizure, but imaging can be done later, when the patient is stable. Since the SPECT tracer is taken up rapidly by the brain and does not significantly redistribute, imaging done later reflects cerebral blood flow (CBF) from the time of the injection during the seizure.

We used SPECT to image spontaneous secondarily generalized tonic–clonic seizures in a relatively large group of patients with epilepsy. We obtained images from the pre-generalization phase, during generalization, or in the post-ictal period, and performed group analyses using statistical parametric mapping (SPM) to identify cortical and subcortical regions most commonly involved. With this approach, we found focal CBF increases in the regions of seizure onset, with later increases in bilateral subcortical networks. Subcortical increases were related through correlation analysis to decreases in the fronto-parietal association cortex, possibly explaining impaired consciousness during and following tonic–clonic seizures.

Methods

Data acquisition

Fifty-nine ictal–interictal SPECT scan pairs were acquired from 53 patients who had secondarily generalized tonic–clonic seizures during continuous video-EEG monitoring. Six patients were injected twice on different days (see below). Patient scans were divided into three groups for analysis: (i) *Pre-generalization*: 12 scans were injected with Tc-99 HMPAO during the partial seizure phase prior to generalization; 5 of these were in patients with left hemisphere seizure onset based on concordance of pre-surgical data and clinical outcome after surgery, 4 had right hemisphere onset and 3 were unlateralized (side of onset unknown based on clinical data); (ii) *Generalization*: 12 scans were injected after onset of generalization and prior to seizure end; 6 with left hemisphere seizure onset, 4 right hemisphere onset and 2 unlateralized; and (iii) *Post-ictal*: 35 scans were injected after seizure termination; 13 left, 11 right hemisphere onset and 11 unlateralized. Of the six patients who were injected twice on different days, one patient had seizures injected in both the pre-generalization and post-ictal period, two had seizures injected in the generalization and post-ictal periods and three had two seizures injected at different times in the post-ictal period. Late injections, including those performed in the post-ictal period were not intentional, but due to limitations in staff and radiopharmaceutical necessary for consistent early injections. Interictal SPECT scans were acquired at least 24 h after the most recent seizure.

SPECT images were acquired within 90 min after injection. Projection data were obtained on a Picker PRISM 3000, 3000XP or Marconi/Philips IRIX 3 headed scanner (Philips Medical Systems, Best, Netherlands) mounted with high resolution fan beam collimators. Transverse slices were reconstructed using standard low pass Butterworth filter and Chang attenuation correction as previously described (Zubal *et al*., 1995).

Localization of seizure onset was determined when possible using concordance of other clinical tests and clinical outcome, as described previously (McNally *et al*., 2005).

Image analysis

Images were analysed using statistical parametric mapping (SPM2, Wellcome Department of Cognitive Neurology, London, UK, http://fil.ion.ucl.ac.uk/spm/) on a MATLAB (The MathWorks, Inc. Natick, MA) platform. Individual patient ictal–interictal SPECT difference analyses were performed using ictal–interictal SPECT analysed by SPM (ISAS), as described in detail previously (Chang *et al*., 2002; McNally *et al*., 2005). This method provides regions of statistically significant SPECT increases and decreases compared with interictal baseline images for each patient. Full details of the ISAS method, including free downloads of the software and databases are available at http://spect.yale.edu/.

Group analyses were performed using a paired *t*-test model in SPM to compare the ictal (or post-ictal) versus interictal images for patients in each group (pre-generalization, generalization and post-ictal). Using the paired *t*-test model, we can make observations within each group and still preserve the ictal–interictal scan pair relationship. As described previously (Blumenfeld *et al*., 2004*a*), images were realigned, spatially normalized, masked and smoothed using a $16 \times 16 \times 16\,mm^3$ Gaussian kernel. Global intensity normalization was performed to correct for differences in total brain counts among scan pairs, using SPM defaults. This involved first calculating a global mean for each image. Then, to avoid effects of zero voxels outside the brain, the mean was recalculated excluding all voxels with intensity values below the initial mean divided by eight. All voxels were then divided by this final mean value and multiplied by 50, resulting in a global mean of ~50 for each brain. After intensity normalization, the image was masked using the SPM analysis threshold default of 0.8, which removes all voxels with intensity <80% of the global mean (usually these are non-grey matter voxels). Contrasts were chosen to detect hyperperfusion and hypoperfusion throughout the entire brain. The extent threshold (k), below which clusters were rejected, was 125 voxels. This is equivalent to a volume of 1cc (with SPM voxel dimensions of $2 \times 2 \times 2\,mm^3$). Individual voxel-level significance threshold P was 0.01, corresponding to a Z-score of 2.33. We further required that clusters of voxels have a corrected cluster-level significance $P < 0.05$ to be considered significant, which effectively corrects for multiple comparisons for the entire brain (Friston *et al*., 1994, 1996; Brett *et al*., 2003). These thresholds were chosen based on our prior epilepsy SPECT investigations (Blumenfeld *et al*., 2003*b*, 2004*a*), including an ROC analysis (McNally *et al*., 2005). When using this approach, SPM displays all clusters exceeding the voxel-level threshold ($P = 0.01$) and extent threshold ($k = 125$), even if they do not meet the corrected cluster level significance threshold ($P = 0.05$). This enables subthreshold changes to be visualized in the data; however, it is necessary to specify in the text and tables which clusters are statistically significant.

Two different approaches were used for the group analyses. Side of seizure onset was known for some, but not all of the patients, based on EEG or other clinical data. Therefore, for group analyses, we initially combined all data from seizures with left, right and unknown side of seizure onset. We refer to this analysis approach below as 'L-R combined'. Group analysis of this kind should reveal regions most commonly involved in CBF increases or decreases regardless of side of seizure onset. As a second approach, we repeated the group analysis with the subset of patients for which side of onset was known based on clinical data ($n = 43$ of 59 scans), but first flipped all images from right-onset seizures (using the spm_flip utility), so that group changes ipsi- or contralateral to onset could be visualized. This second approach is referred to below as 'lateralized'. Using these two approaches includes the advantages of both maximizing sample size (L-R combined analysis, $n = 59$) and examining unilateral changes with smaller sample size (lateralized analysis, $n = 43$).

To study the timecourse of SPECT changes in the cerebellum, and to perform correlation analyses, we used the number of voxels (k) showing significant changes as an approximate measure of the amount of change in this structure. A binary volume corresponding to the cerebellum was created manually in MRIcro (http://www.psychology.nottingham.ac.uk/staff/cr1/mricro.html), using the SPM MRI template Colin27 (see http://www.mrc-cbu.cam.ac.uk/Imaging/mnispace.html and ftp://ftp.mrc-cbu.cam.ac.uk/pub/imaging/Colin/). The total number of voxels showing significant hypoperfusion and hyperperfusion (at a voxel-level significance threshold $P = 0.01$, and cluster-extent threshold $k = 125$ as before) were then determined in the cerebellum for each patient from their ISAS analysis, using the small volume correction function in SPM. All seizures ($n = 59$) were included in this analysis.

To analyse the partial correlation between cerebellar changes and changes in all other brain regions, we performed an SPM analysis using the multi-subject, conditions and covariates model, entering the total number of cerebellar hyperperfusion voxels for each patient (determined above) as the covariate. For this analysis, we again used an extent threshold $k = 125$ voxels, and voxel-level significance threshold $P = 0.01$, followed by a cluster-level significance threshold

$P = 0.05$ corrected for the entire brain, and all seizures ($n = 59$) were included.

Behavioural analysis

Video and EEG of seizures for all SPECT injections were reviewed by two readers, blinded to the results of the imaging studies. Seizure onset was defined as the earliest EEG or clinical evidence of seizure activity. Seizure offset was defined as the last EEG or clinical evidence of seizure activity; usually this coincided with the last clonic jerk exhibited by the patient. Onset of generalization was defined based on head or eye version, vocalization or asymmetric tonic facial contraction, as in previous behavioural studies of generalized tonic–clonic seizures (Theodore *et al*., 1994; Jobst *et al*., 2001). SPECT injection time was defined as when the plunger of the syringe containing the radiopharmaceutical was fully depressed.

Level of consciousness was evaluated during the 30s following SPECT injection based on responses to external stimulation, questions or commands. Motor activity during this 30s period was also described based on video review for each patient. Analysis of the severity of the tonic phase (even if not during this 30s period) was performed for all patients based on previous criteria (Theodore *et al*., 1994; Jobst *et al*., 2001) with a scale from 0 to 4, with 0 indicating no tonic activity, and 4 signifying motionless contraction during the tonic phase.

Results

Cortical and subcortical CBF increases

Secondarily generalized tonic–clonic seizures were associated with early functional imaging changes in the regions of seizure onset, followed by bilateral cortical and subcortical changes in specific networks. We analysed SPECT images from 59 seizures in 53 patients injected during three different time epochs: during the partial seizure phase prior to generalization (pre-generalization; $n = 12$), during the generalization phase ($n = 12$) and post-ictally ($n = 35$).

In the pre-generalization phase, analysis of individual patients demonstrated focal CBF increases in different regions related to the variable anatomical locations of seizure onset (data not shown). Focal CBF increases from these brain regions cancelled out in the L-R combined group analysis, and the subthreshold increases seen in the temporal lobes did not reach significance at the cluster level (Fig. 1A and 2A; Table 1).

During the generalization phase, similarly, focal but variable cortical increases were seen in individual patients tending to cancel out in the L-R combined group analysis, which resulted in no significant overall cortical increases. However, consistent CBF increases in several important subcortical structures emerged in the group analysis of generalization (Fig. 1B and 2B; Table 1). Thus, significant hyperperfusion was observed in the superior medial cerebellum, as well as in the left thalamus and basal ganglia during the generalization phase. Increases in the right thalamus and basal ganglia formed a separate cluster which did not reach statistical significance. The increases seen in the cerebellum, basal ganglia and thalamus are consistent with the known important role of these subcortical structures in seizure generalization (Avoli *et al*., 1990; Gale, 1992; Norden and Blumenfeld, 2002).

While CBF increases are expected with the intense neuronal activity during seizures, we were surprised to observe that in the post-ictal phase following generalized tonic–clonic seizures, a massive CBF increase was seen involving almost the entire cerebellum (Fig. 1C and 2C; Table 1). This cerebellar hyperperfusion was analysed in greater detail, as we will describe shortly. CBF increases in the post-ictal period were also observed in the midbrain, but increases in the caudate and adjacent white matter did not reach cluster-level significance (Fig. 1C and 2C; Table 1).

These L-R combined group analyses included both left- and right-onset seizures, so that unilateral changes may be lost in the average. To determine the possible influence of unilateral onset on our results, we repeated the above analyses with the subset of patients for whom side of seizure onset was known. Scans from patients with right-sided onset were flipped right-left (using the spm_flip utility) and combined with left-sided onset patients to yield maps of changes ipsi- and contralateral to seizure onset. When group analyses were repeated with this lateralized approach, we found generally similar regions of CBF increases to analyses with non-flipped (L-R combined) images, with some differences. Thus, in the pre-generalization group ($n = 9$ with known side of onset; five left, four right), there were significant increases in the ipsilateral temporal cortex in the lateralized analysis (Fig. 3A and 4A; Table 2). This agrees with the fact that the temporal lobes were most consistently involved in seizure onset (6 of 12 patients in this group had confirmed temporal lobe onset). In the generalization group ($n = 10$, 6 left-sided onset, 4 right), there were significant increases in the bilateral superior medial cerebellum; and in the post-ictal group ($n = 24$; 13 left, 11 right), there were more dramatic increases in the bilateral cerebellum and midbrain, and ipsilateral caudate (Fig. 3 and 4; Table 2). Overall, the lateralized analysis showed some focal cortical CBF increases during the pre-generalization phase (in regions of onset). This was followed by mainly bilateral subcortical increases at later times, similar to those seen in the larger L-R combined group analysis.

CBF decreases and behavioural changes

CBF decreases were also observed in specific regions of the cerebral cortex during and following secondarily generalized tonic–clonic seizures. In the pre-generalization phase, with L-R combined analysis we observed CBF decreases in the cingulate gyrus and frontal cortex (Fig. 1A and 2A; Table 1). These decreases became more pronounced during generalization (Fig. 1B and 2B; Table 1), and evolved to profound hypoperfusion in the post-ictal period involving the orbital frontal, lateral frontal, anterior cingulate as well as posterior cingulate cortices (Fig. 1C and 2C; Table 1).

To determine if the observed SPECT changes may be correlated with impaired consciousness, we analysed behaviour during and following seizures in all patients based on video recordings, looking particularly at behaviour during the first 30s following SPECT injection, since most of the radiopharmaceutical is taken up by the brain during this interval (Andersen, 1989; Devous *et al*., 1990). For injections in the pre-generalization and generalization phases, patients exhibited the characteristic motor behaviours associated

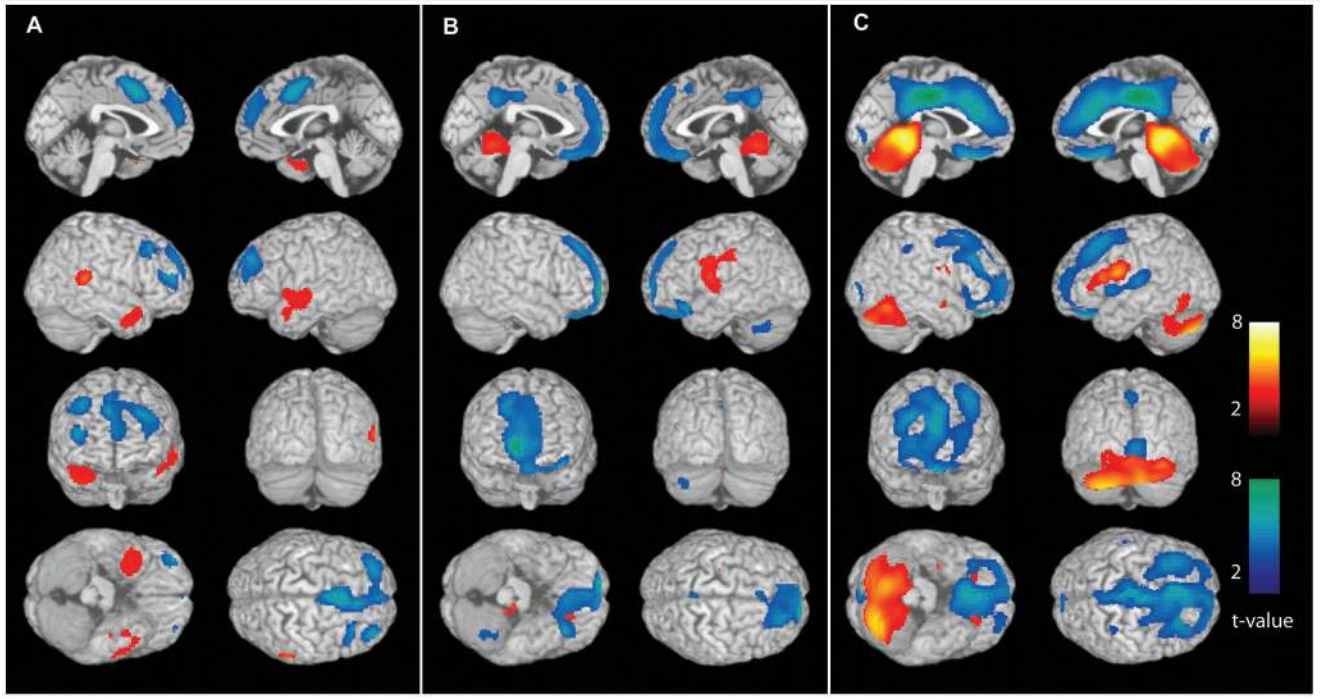

Figure 1 Secondarily generalized tonic–clonic seizures are associated with CBF changes in cortical and subcortical networks. Data from L-R combined analyses are shown (see 'Methods' section). Statistical parametric maps depict CBF increases (warm colours) and decreases (cool colours) compared with baseline interictal images. (**A**) Pre-generalization period ($n = 12$). Increases in the temporal lobes (the most common region of seizure onset) do not reach statistical significance at the cluster level, while significant decreases occur in the cingulate gyrus and frontal association cortex. (**B**) Generalization period ($n = 12$). Significant increases at the cluster level occur in the superior medial cerebellum, left thalamus and basal ganglia, while significant decreases occur in the frontal association cortex. Note that thalamic and basal ganglia increases are not visible in these surface renderings (see Fig. 2B for subcortical changes) except for where they artifactually appear on the lateral surface in the second row, right image (left lateral brain view). In fact, no significant cortical increases occur in the group analysis during the generalization period (Fig. 2B, Table 1). (**C**) post-ictal period ($n = 35$). Significant increases occur in the cerebellum and dorsal midbrain, while decreases occur in the frontal association cortex, cingulate and precuneus. As in the generalization period, no significant cortical increases occur, but some of the basal ganglia signal appears on the lateral surface due to the surface rendering algorithm. For **A–C**, extent threshold, $k = 125$ voxels (voxel size = $2 \times 2 \times 2\,mm^3$). Height threshold, $P = 0.01$. Equivalently, only voxel clusters greater than 1 cm^3 in volume and with Z scores greater than 2.33 are displayed. Only regions with corrected $P < 0.05$ are considered significant at the cluster level (Table 1).

with secondarily generalized tonic–clonic seizures (Theodore *et al*., 1994; Jobst *et al*., 2001), including facial clonus, vocalization, head version, tonic and clonic limb movements. Of the 35 patients injected in the post-ictal period, most lay still with eyes closed breathing deeply, nine resumed some spontaneous movements within 30 s of injection including agitation in two and moaning vocalizations in two patients. All patients injected post-ictally were deeply unresponsive to questions, commands and other external stimuli during this time, except for one patient who regained the ability to speak, but was disoriented.

As with CBF increases, we repeated the analysis using only patients with known side of onset, and flipped images of right-onset seizures prior to group analysis. This allowed us to visualize CBF decreases ipsi- or contralateral to side of onset. With this lateralized approach, in the pre-generalization group ($n = 9$; five left-sided onset, four right), there were again CBF decreases in the bilateral cingulate and frontal cortex, which became more pronounced in the generalization group ($n = 10$, six left-sided onset, four right), and evolved to dramatic bilateral hypoperfusion of the orbital frontal, anterior and posterior cingulate, and contralateral fronto-parietal cortex in the post-generalization group ($n = 24$; 13 left, 11 right) (Fig. 3 and 4; Table 2). These findings were again in general agreement with the larger L-R combined group analyses that included all patients (Fig. 1, 2 and Table 1), but showed some lateralization of late fronto-parietal CBF decreases to the side contralateral to onset.

Cerebellar timecourse and network correlations

Because we observed large unexpected post-ictal CBF increases in the cerebellum, we analysed ictal and post-ictal cerebellar CBF changes in greater detail. The aggregate timecourse was estimated by measuring the total number of voxels showing significant cerebellar CBF changes for individual patients injected at different times (Fig. 5; $n = 59$). This analysis demonstrated that cerebellar hyperperfusion tended to increase progressively with later injection times in the post-ictal period. A similar pattern of progressive

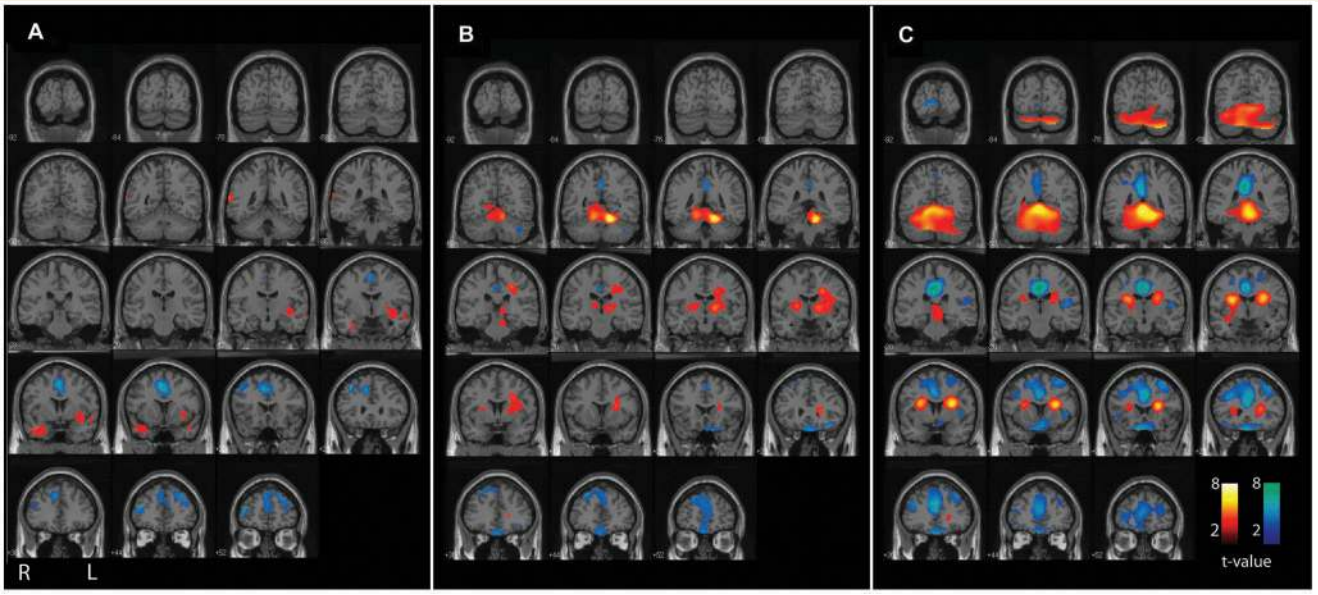

Figure 2 CBF changes associated with secondarily generalized tonic–clonic seizures (L-R combined analysis), with results overlaid on a structural MRI in the coronal plane. Same patients and data are shown as in Fig. 1. Statistical parametric maps depict CBF increases (warm colours) and decreases (cool colours) compared with baseline interictal images. (**A**) Pre-generalization period ($n = 12$). Increases in the temporal lobes (the most common region of seizure onset) do not reach cluster-level significance (Table 1), while significant decreases occur in the cingulate gyrus and frontal association cortex. (**B**) Generalization period ($n = 12$). Significant increases at the cluster level occur in the superior medial cerebellum, left thalamus and basal ganglia, while significant decreases occur in the frontal association cortex. (**C**) post-ictal period ($n = 35$). Significant increases occur in the cerebellum and midbrain, while decreases occur in the frontal association cortex, cingulate and precuneus. Increases in basal ganglia and adjacent white matter do not reach cluster-level significance. For **A**–**C**, extent threshold, $k = 125$ voxels (voxel size = $2 \times 2 \times 2\,mm^3$). Height threshold, $P = 0.01$. Equivalently, only voxel clusters greater than $1\,cm^3$ in volume and with Z scores greater than 2.33 are displayed. Only regions with corrected $P < 0.05$ are considered significant at the cluster level (Table 1).

Table 1 Significant changes in generalized tonic–clonic seizures: L-R combined analysis ($n = 59$)

Brain regions[a]	Corrected cluster significance, P[b]	Cluster volume, k[c]	Location of most significant voxel	x, y, z[d]	Z-score[e]
Pre-generalization					
Hyperperfusion					
No significant clusters	–	–	–	–	–
Hypoperfusion					
Bilateral cingulate, bilateral superior frontal gyrus	0.013	3885	Right cingulate gyrus	−4, 12, 46	3.74
Generalization					
Hyperperfusion					
Bilateral superior cerebellum, left thalamus, left caudate	<0.001	7508	Left superior cerebellum	16, −50, −20	4.46
Hypoperfusion					
Bilateral anterior medial frontal, bilateral orbitofrontal	0.002	4919	Right anterior medial frontal	−14, 64, 0	4.39
Post-ictal					
Hyperperfusion					
Bilateral cerebellum, midbrain	<0.001	15 893	Superior vermis	−2, −46, −4	5.42
Hypoperfusion					
Bilateral orbitofrontal, bilateral middle frontal gyrus, bilateral cingulate, bilateral precuneus	<0.001	19 997	Midline posterior cingulate	0, −18, 40	6.01

Same data as in Fig. 1 and 2.
a Location of clusters with voxel-level significance $P < 0.01$, extent $k > 125$, and corrected cluster-level significance $P < 0.05$.
b P = cluster-level significance corrected for multiple comparisons for the entire brain.
c k = cluster size in voxels (voxel size = $2 \times 2 \times 2$ mm).
d x, y, z are coordinates in MNI space of the most significant voxel (maximum Z-score) for the cluster.
e Z_E score for most significant voxel in the cluster.

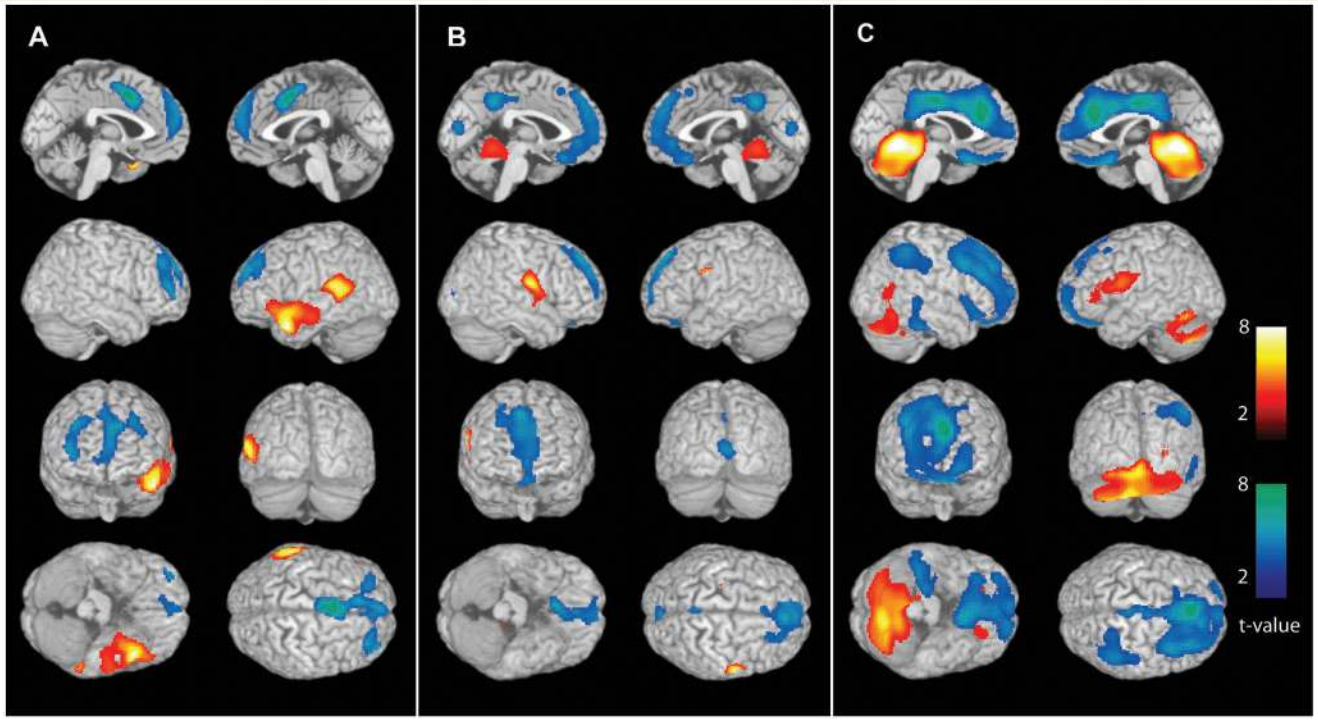

Figure 3 CBF changes ipsi- and contralateral to side of seizure onset in secondarily generalized tonic–clonic seizures (lateralized analysis). Changes ipsilateral to seizure onset are shown on the left side of the brain rendering, and contralateral changes on the right side of the brain (combining patients with left- and right-onset seizures). CBF increases (warm colours) and decreases (cool colours) were analysed compared with baseline interictal images. (**A**) Pre-generalization period ($n = 9$). Significant increases occur in the ipsilateral temporal lobe (the most common region of seizure onset), while decreases occur in the bilateral cingulate gyrus and frontal association cortex. (**B**) Generalization period ($n = 10$). Significant increases occur in the bilateral superior medial cerebellum. Increases seen in thalamus, basal ganglia and contralateral Rolandic cortex did not reach significance at the cluster level. Significant decreases occur in the bilateral frontal association cortex (slightly more pronounced contralateral). (**C**) post-ictal period ($n = 24$). Significant increases occur in the bilateral cerebellum, midbrain and ipsilateral basal ganglia, while decreases occur in the bilateral frontal association cortex (more pronounced contralateral), bilateral cingulate and precuneus, and in the contralateral lateral parietal cortex. No significant cortical increases occur post-ictally, but some of the basal ganglia signal appears on the lateral surface (second row of images) due to the surface rendering algorithm. For **A–C**, extent threshold, $k = 125$ voxels (voxel size = $2 \times 2 \times 2\,mm^3$). Height threshold, $P = 0.01$. Equivalently, only voxel clusters greater than $1\,cm^3$ in volume and with Z scores greater than 2.33 are displayed. Only regions with corrected $P < 0.05$ are considered significant at the cluster level (Table 2).

post-ictal increases was seen if either the left or right half of the cerebellum was analysed separately (data not shown). CBF decreases in the cerebellum did not show this pattern of temporal evolution (Fig. 5).

To further investigate the spatial evolution of these changes in different anatomical regions of the cerebellum, we subdivided the post-ictal injections into early (0–30 s), intermediate (30–60 s) and late (>60 s) times following seizure end (Fig. 6). In the pre-generalization period, no significant cerebellar increases were seen in the group analysis. During generalization, cerebellar hyperperfusion was present mainly in the region of the superior medial cerebellum and deep cerebellar nuclei. At early (0–30 s; $n = 12$) times after seizure end, these increases in the superior midline cerebellum became more pronounced. At intermediate (30–60 s; $n = 13$) and late (>60 s; $n = 10$) times, there was a striking shift of hyperperfusion into the lateral cerebellar hemispheres, with midline regions less involved (Fig. 6).

Aside from the relationship between cerebellar hyperperfusion and time of injection (Fig. 5 and 6), we did not find any relationship between cerebellar hyperperfusion and other behavioural features of the seizures. Thus, the amount of cerebellar hyperperfusion was not related to total seizure duration (mean 126 s; range 40–486 s), duration of the tonic phase (mean 25 s; range 8–59 s), duration of the clonic phase (mean 31 s; range 7–130 s) or to severity of the tonic contractions (mean tonic rating = 3.17; range 0–4) as determined by video review based on previously established behavioural criteria (Theodore *et al*., 1994; Jobst *et al*., 2001).

Since the cerebellum has well-known reciprocal network connections with other brain regions, including the cerebral cortex via thalamus and pons, we were interested in determining whether changes in other brain regions were correlated with CBF changes in the cerebellum. To investigate this, we performed a correlation analysis in SPM between CBF changes in the cerebellum, and all brain regions, across all 59 seizures. This analysis enabled us to determine which regions showed significant relationships with changes in the cerebellum, and whether they were positively or negatively associated with cerebellar changes. Significant positive

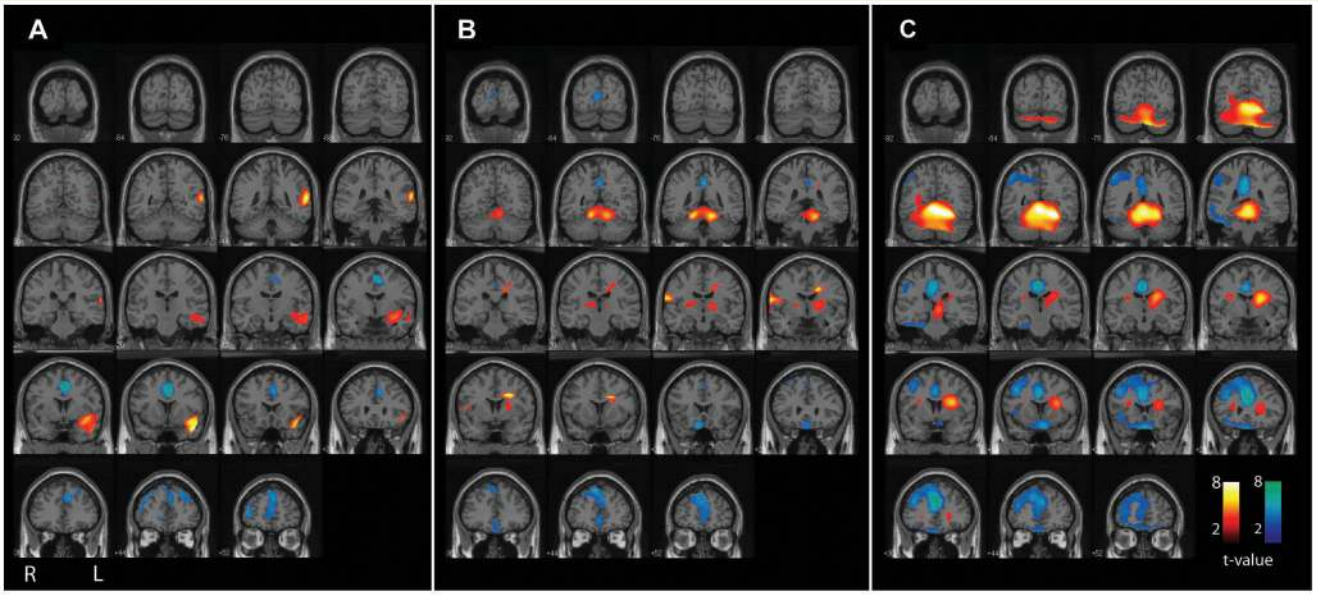

Figure 4 CBF changes ipsi- and contralateral to side of seizure onset (lateralized analysis) overlaid on a structural MRI in the coronal plane. Same patients and data are shown as in Fig. 3. Changes ipsilateral to seizure onset are shown on the left side of the brain sections, and contralateral changes on the right side (combining patients with left- and right-onset seizures). CBF increases (warm colours) and decreases (cool colours) were analysed compared with baseline interictal images. (**A**) Pre-generalization period ($n = 9$). Significant increases occur in the ipsilateral temporal lobes (the most common region of seizure onset), while decreases occur in the bilateral cingulate gyrus and anterior medial frontal association cortex. (**B**) Generalization period ($n = 10$). Significant increases occur in the bilateral superior medial cerebellum. Increases seen in thalamus, basal ganglia and contralateral Rolandic cortex did not reach significance at the cluster level. Significant decreases occur in the bilateral frontal association cortex (slightly more pronounced contralateral). (**C**) Post-ictal period ($n = 24$). Significant increases occur in the bilateral cerebellum, midbrain, ipsilateral basal ganglia and adjacent white matter, while decreases occur in the bilateral frontal association cortex (more pronounced contralateral), bilateral cingulate and precuneus, and in the contralateral lateral parietal cortex. For **A–C,** extent threshold, $k = 125$ voxels (voxel size $= 2 \times 2 \times 2\,mm^3$). Height threshold, $P = 0.01$. Equivalently, only voxel clusters $>1\,cm^3$ in volume and with *Z*-scores greater than 2.33 are displayed. Only regions with corrected $P < 0.05$ are considered significant at the cluster level (Table 2).

correlations were found between the cerebellum, thalamus and upper brainstem tegmentum including the midbrain and pons [Fig. 7; cluster-level $P < 0.0001$ corrected for multiple comparisons, $k = 21\,834$ (voxel dimensions $2 \times 2 \times 2\,mm^3$), maximum voxel $t = 13.64$]. Interestingly, significant correlations were also found between cerebellar hyperperfusion, and hypoperfusion in specific regions of the higher-order association cortex, including the bilateral lateral prefrontal cortex, orbital frontal cortex, lateral parietal cortex, anterior cingulate and posterior cingulate/precuneus regions (Fig. 7; cluster-level $P < 0.0001$ corrected for multiple comparisons, $k = 27\,909$, maximum voxel $t = 6.29$). Therefore, cerebellar increases were related to other network changes including increases in the thalamus and brainstem, and decreases in the fronto-parietal association cortex.

Discussion

We observed that secondarily generalized tonic–clonic seizures are associated with variable focal CBF increases in the cortex of individual patients. However, group analysis revealed consistent subcortical increases which are correlated with decreased CBF in the fronto-parietal association cortex. For SPECT injections performed during the pre-generalization period, group analysis revealed focal CBF increases mainly in the temporal lobes, reflecting the most common region of partial seizure onset. During generalization, there were CBF increases in the thalamus, basal ganglia and superior medial cerebellum, and post-ictally, progressive CBF increases were observed in the cerebellar hemispheres and midbrain. The marked CBF increases in the cerebellum were correlated with increases in the midbrain and thalamus, and were also correlated with decreases observed in the fronto-parietal association cortex. Nearly all patients were deeply unconscious at the time of SPECT injection. These results allow us to describe a network of cortical and subcortical structures which could play a crucial role in the generation and behavioural manifestations of secondarily generalized tonic–clonic seizures.

Focal cortical changes in generalized seizures, with intense involvement of specific brain regions and relative sparing of others, have been observed in both generalized tonic–clonic seizures (Blumenfeld *et al*., 2003*a*, 2003*b*; Enev *et al*., 2007; Schindler *et al*., 2007; Varghese *et al*., 2008) and in absence seizures (Meeren *et al*., 2002; Archer *et al*., 2003; Aghakhani *et al*., 2004; Nersesyan *et al*., 2004; Berman *et al*., 2009;

Table 2 Significant changes in generalized tonic–clonic seizures: lateralized analysis ($n = 43$)

Brain regions[a]	Corrected cluster significance P[b]	Cluster Volume, k[c]	Location of most significant voxel	x, y, z[d]	Z-score[e]
Pre-generalization					
Hyperperfusion					
Ipsilateral anterior temporal	0.011	2858	Ipsilateral anterior temporal	48, 12, −28	4.12
Hypoperfusion					
Bilateral anterior cingulate, bilateral medial anterior frontal	0.003	3650	Midline cingulate	0, 4, 46	4.00
Generalization					
Hyperperfusion					
Bilateral superior cerebellum	0.017	2838	Contralateral superior cerebellum	−16, −48, −16	4.03
Hypoperfusion					
Bilateral anterior medial frontal, bilateral orbitofrontal	0.006	3613	Contralateral oribital frontal	−8, 20, −20	3.70
Post-ictal					
Hyperperfusion					
Bilateral cerebellum, midbrain, ipsilateral caudate, ipsilateral white matter	<0.001	19 179	Ipsilateral cerebellum	26, −52, −16	6.21
Hypoperfusion					
Bilateral orbitofrontal, contralateral middle frontal gyrus, bilateral cingulate, bilateral precuneus, contralateral lateral parietal	<0.001	19 610	Midline anterior cingulate	2, 34, 28	5.23

Same data as in Fig. 3 and 4.
a Location of clusters with voxel-level significance $P < 0.01$, extent $k > 125$ and corrected cluster-level significance $P < 0.05$.
b P = cluster-level significance corrected for multiple comparisons for the entire brain.
c k = cluster size in voxels (voxel size = 2 × 2 × 2 mm).
d x, y, z are coordinates in MNI space of the most significant voxel (maximum Z-score) for the cluster.
e Z_E score for most significant voxel in the cluster.

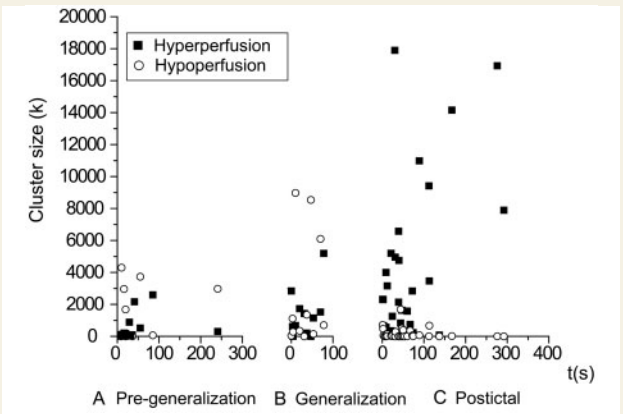

Figure 5 Cerebellum shows progressive CBF increases in the post-ictal period following secondarily generalized tonic–clonic seizures. Total number of cerebellar voxels with significant CBF increases (filled square) or decreases (open circle) in individual patients are plotted against SPECT injection time. (**A**) Pre-generalization ($n = 12$). (**B**) Generalization ($n = 12$). (**C**) Post-ictal ($n = 35$). Time = 0 in each case is the beginning of the pre-generalization, generalization or post-ictal epochs. Patients were the same as in Fig. 1 and 2. Analysis was performed using the small volume correction in SPM to identify significant SPECT changes in the cerebellum of individual patients at a voxel-level significance threshold $P = 0.01$, and cluster-extent threshold $k = 125$ (see 'Methods' section for details).

Hamandi *et al*., 2008; Moeller *et al*., 2008). The importance of these focal changes in 'generalized seizures' and their role in seizure generation and in behavioural manifestations have been discussed at length elsewhere (Blumenfeld *et al*., 2003*b*; Blumenfeld, 2005*a*, 2003*b*; Meeren *et al*., 2005; Varghese *et al*., 2009). In the present study, group analysis has eliminated most of the variable focal cortical changes except for in the pre-generalization period. The focal temporal lobe increases seen in the pre-generalization group resembled those seen at the site of seizure initiation during induced tonic–clonic seizures in prior work (Enev *et al*., 2007).

The group analysis enabled us to identify the most consistently involved regions across patients despite variable focal onset. Interestingly, although focal or unilateral cortical changes were seen in the pre-generalization, generalization, and even post-ictal periods in analyses of individual patients (Varghese *et al*., 2009), the group analysis demonstrated increases mainly in subcortical structures. In the cerebral cortex, variable focal CBF increases cancelled out in the group analysis, except for in unilateral analysis of the pre-generalization period. However, consistent bilateral CBF decreases were seen in the fronto-parietal association cortex during and following seizures. In addition, subcortical increases were present which became progressively more prominent, especially in the cerebellum, in the post-ictal period. The post-ictal changes differed in this respect from other states of impaired consciousness, such as slow wave sleep, in which cortical CBF decreases are seen without increases in the cerebellum

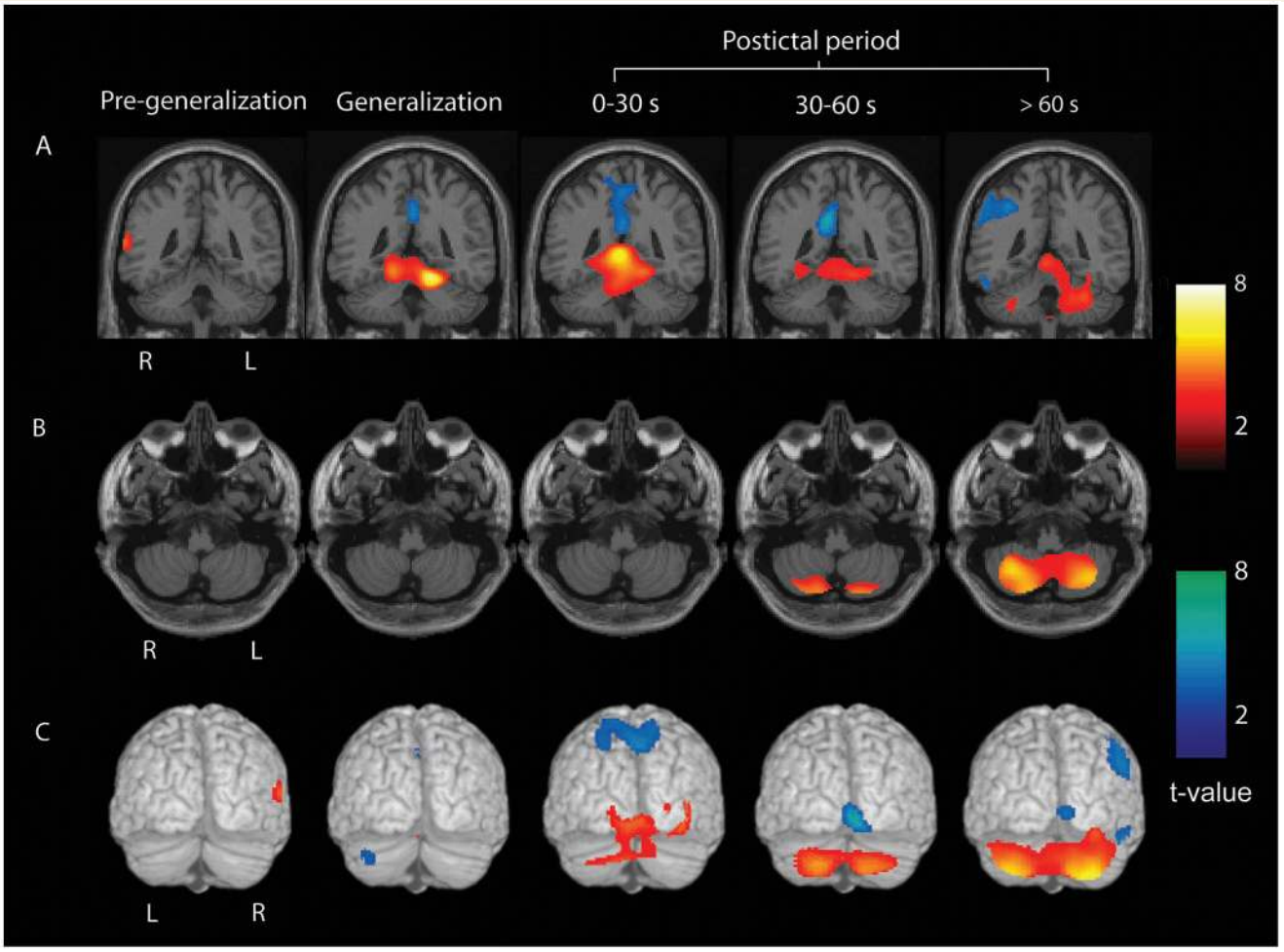

Figure 6 Evolution of cerebellar CBF increases from the superior medial cerebellum to the lateral cerebellar hemispheres. Statistical parametric maps depict CBF increases (warm colours) and decreases (cool colours) compared with baseline interictal images. (**A**) CBF increases and decreases overlaid on a structural MRI in the coronal plane demonstrates superior medial cerebellar increases peaking during the generalization and early post-ictal (0–30 s) periods. (**B**) Axial sections through the inferior cerebellum demonstrating lateral cerebellar increases most prominent at late post-ictal times (>60 s). (**C**) Posterior surface renderings demonstrating medial to lateral evolution of cerebellar CBF increases during the post-ictal period. (**A–C)** Group analyses were performed for SPECT injections during the pre-generalization ($n = 12$), generalization ($n = 12$), early post-ictal (0–30 s, $n = 12$), middle post-ictal (30–60 s, $n = 13$) and late post-ictal (>60 s, $n = 10$) periods. Patients were the same as in Fig. 1 and 2. SPM extent threshold, $k = 125$ voxels (voxel size = $2 \times 2 \times 2\ mm^3$). Height threshold, $P = 0.01$.

(Dang-Vu *et al*., 2005). It is also notable that we observed both increases and decreases in CBF at times after the abrupt cessation of the widespread neuronal discharge on EEG defining the end of the seizure. This suggests either a dissociation of CBF changes and neuronal events, or continued neuronal events not accessible to conventional EEG recordings.

One possible concern with group analysis, which combines both left- and right-onset seizures, is that unilateral changes would be lost in the average. To address this, we repeated the group analysis with the subset of patients in which side of onset was known using a lateralized approach, analysing all seizures based on changes ipsi- or contralateral to the side of onset. Interestingly, the lateralized analysis still showed mainly subcortical increases and bilateral cortical decreases. There were some minor differences between the L-R combined and lateralized analyses. For example, the lateralized analysis showed significant increases in the ipsilateral temporal lobe in the pre-generalization period, presumably due to better lateralization of changes, which in the L-R combined analysis were distributed bilaterally and did not reach significance. On the other hand, thalamic increases in the generalization period reached significance only in the L-R combined analysis (and in the correlation analysis), while thalamic changes in the lateralized analysis did not reach significance, likely due to smaller sample size. However, overall both analyses showed bilateral increases during the generalization and post-ictal periods particularly in the cerebellum, and bilateral decreases in fronto-parietal association cortex. The bilateral changes in these structures may be important for the bilateral behavioural features seen in generalized tonic–clonic seizures. This supports a model in which focal activity increases in the cerebral cortex trigger subcortical increases and

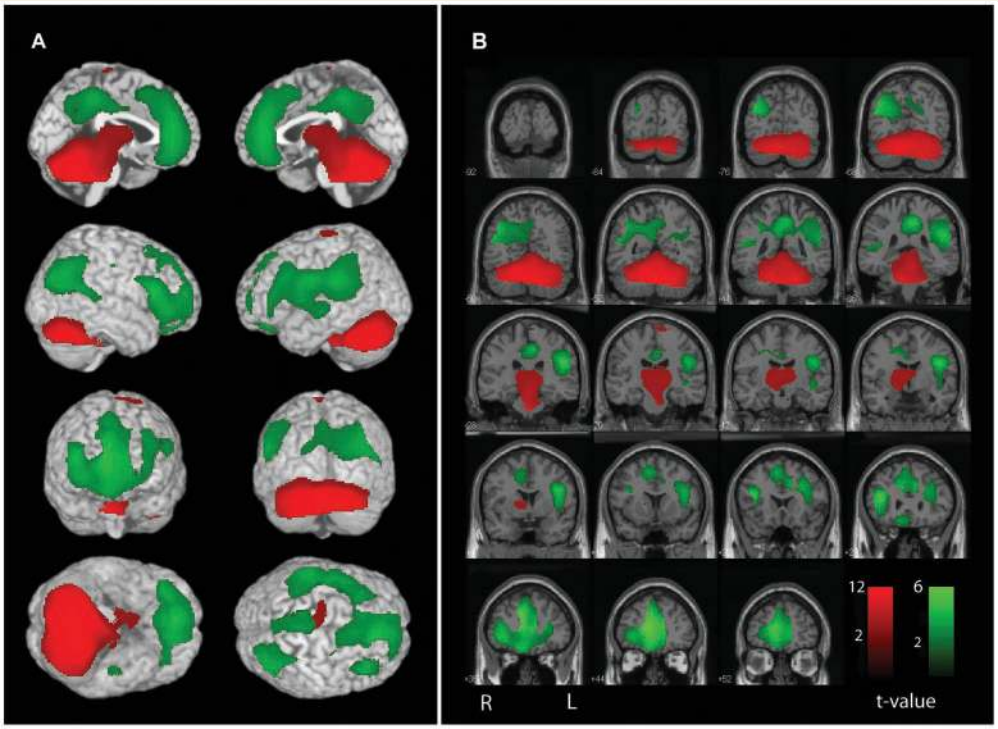

Figure 7 Network correlations between cerebellar CBF changes and other brain regions. Positive (red) and negative (green) correlations are shown. SPM analysis was used to correlate SPECT changes in the cerebellum with all voxels in the brain across patients ($n = 59$). (**A**) Surface rendering. (**B**) Coronal sections. Significant positive correlations with cerebellar CBF changes were found in the upper brainstem tegmentum and thalamus. Negative correlations were found with the bilateral fronto-parietal association cortex, anterior and posterior cingulate and precuneus. Patients were the same as in Fig. 1 and 2. SPM extent threshold, $k = 125$ voxels (voxel size $= 2 \times 2 \times 2\,mm^3$). Height threshold, $P = 0.01$.

cortical decreases in activity, which may underlie the pathophysiology of secondary generalization.

Much previous work supports an important role for the thalamus and upper brainstem in generalized seizures (Kreindler *et al*., 1958; Browning and Nelson, 1986; Avoli *et al*., 1990; Jasper, 1991; Gale, 1992; Miller, 1992; Faingold, 1999; Blumenfeld, 2002; Norden and Blumenfeld, 2002). These structures are thought to be critical for synchronizing abnormal cortical–subcortical electrical discharges, for generating tonic motor activity, and for producing impaired consciousness in epilepsy. Involvement of the upper brainstem and thalamus in human secondarily generalized seizures supports the proposed role of these structures in seizure generalization. The basal ganglia have been shown to play an important role in the regulation of seizures (McNamara *et al*., 1984; Gale, 1992) and in ictal dystonia (Kotagal *et al*., 1989; Newton *et al*., 1992). We observed involvement of the caudate nucleus during the generalization and post-ictal periods, compatible with abnormal increased activity in the basal ganglia during secondarily generalized seizures.

One of the more surprising results in the present study was the marked and progressive increase in CBF we saw in the cerebellum, beginning in the superior medial cerebellum during generalization, and spreading to involve the bilateral lateral cerebellar hemispheres in the post-ictal period. Prior studies have supported a role for the cerebellar cortex and medial deep cerebellar nuclei in tonic motor activity during seizures (Davidson and Barbeau, 1975; Fraioli and Guidetti, 1975; Raines and Anderson, 1976). Continued CBF increases in the cerebellum after the termination of seizures could have several potential mechanisms. One possibility is a primary vascular mechanism, involving some form of reactive vasodilation independent of neuronal activity. Alternatively, continued neuronal activity in the cerebellum after termination of motor seizures could produce increased CBF through neurovascular coupling. Prior work from a cat model (Salgado-Benitez *et al*., 1982) has shown a similar pattern of increased Purkinje cell firing in the medial cerebellum during seizures, which evolved to increased activity in the lateral cerebellum in the post-ictal period. This work supports the likelihood of a primary neuronal mechanism for the cerebellar CBF increases we observed in the ictal and post-ictal periods. Since Purkinje cell outputs are inhibitory, and project via the deep cerebellar nuclei and thalamus to the cerebral cortex, it can be postulated that increased cerebellar activity may contribute to seizures termination and/or to post-ictal suppression (Salgado-Benitez *et al*., 1982). Other studies also support the potential importance of the cerebellum in human epilepsy and in suppression of generalized seizures (Norden and Blumenfeld, 2002; Parmeggiani *et al*., 2008). Because of the known inhibitory role of the cerebellum, cerebellar stimulation has been attempted as a treatment for epilepsy, with initially promising results (Cooper, 1973; Cooper

et al., 1978), although subsequent trials were disappointing (Wright *et al*., 1984). The present results showing marked cerebellar involvement in tonic–clonic seizures suggest that it may be worthwhile to revisit therapies directed at cerebellar targets.

Consistent with the inhibitory outputs of the cerebellum, we found that increased cerebellar activity during and following tonic–clonic seizures was strongly correlated with markedly decreased CBF in the fronto-parietal association cortex. The regions of decreased CBF included the lateral fronto-parietal association cortex, as well as the cingulate gyrus and precuneus. These regions closely resembled the 'default mode' areas reported previously to show decreased activity on functional neuroimaging during normal task performance, and postulated to play an important role in normal attention and consciousness (Raichle *et al*., 2001; Greicius *et al*., 2003;). These same regions have been shown to exhibit markedly decreased activity in other seizure types in which consciousness is impaired including absence seizures (Archer *et al*., 2003; Gotman *et al*., 2005; Laufs *et al*., 2006; Berman *et al*., 2009), and temporal lobe complex partial seizures (Blumenfeld *et al*., 2004*a*, *b*). Of note, the patients in the present study were deeply unresponsive based on video review of their behaviour at the time of SPECT injections.

We have previously proposed a 'network inhibition hypothesis' (or network disruption hypothesis or ictal diaschesis) for loss of consciousness in epilepsy (Blumenfeld, 2005*b*, 2009; Norden and Blumenfeld, 2002; Blumenfeld and Taylor, 2003). According to this hypothesis, despite differences between absence, complex partial and tonic–clonic seizures they all share common anatomical substrates for impaired consciousness. We propose that abnormal increased activity in the thalamus and upper brainstem in all three seizure types disrupts the midline arousal systems, and prevents normal activation of the cortex. This leads to abnormally reduced function in the 'default mode' areas of the fronto-parietal association cortex, and causes impaired consciousness. Support for this hypothesis comes from studies of temporal lobe complex partial seizures, demonstrating that abnormal increases in CBF in the medial thalamus during seizures are correlated with reduced CBF in fronto-parietal association cortex (Blumenfeld *et al*., 2004*a*). Electrophysiological studies in humans (Blumenfeld *et al*., 2004*b*) and animal models (Englot *et al*., 2008) have shown that the regions of association cortex with decreased CBF exhibit large amplitude slow waves resembling coma or deep sleep (but not seizure activity) during hippocampal seizures. These findings suggest that limbic seizures exert remote depressive effects on the neocortex through disruption of midline subcortical networks.

In the present study, we found that increased activity in the cerebellum, midbrain and thalamus was highly intercorrelated, and that increases in these regions were strongly related to decreased CBF in the fronto-parietal default mode regions. The mechanisms for fronto-parietal CBF decreases in secondarily generalized tonic–clonic seizures are not known. Although a hemodynamic mechanism such as vascular steal could contribute, we do not believe that steal is the main mechanism since the CBF decreases occur in different vascular territories from the largest CBF increases, and the decreases also persist or become more pronounced in the post-ictal period when cortical increases are less prominent. We can speculate that, like in temporal lobe seizures, the fronto-parietal association cortex has reduced function during and following tonic–clonic seizures caused by indirect disruption of the midline subcortical arousal systems. In addition, direct disruption of neocortical function by local seizure activity likely also contributes to impaired consciousness during tonic–clonic seizures. Furthermore, the marked bilateral increase in cerebellar outputs may play an important role in depressing fronto-parietal function during tonic–clonic seizures and in the post-ictal period.

In summary, we found that secondarily generalized tonic–clonic seizures exhibit a sequence of subcortical increases and cortical decreases on SPECT imaging, which we hypothesize may be related to ictal and post-ictal behaviours including abnormal motor activity and impaired consciousness. Improved understanding of the specific networks underlying human tonic–clonic seizures may help elucidate targets for new modes of therapy to prevent or to interrupt these most dangerous of all seizures.

Acknowledgements

We thank Sarah Doernberg and Kathryn Davis for initial patient identification and video/EEG review, and Matthew DeSalvo for helpful comments on the manuscript.

Funding

National Instittues of Health (R01 NS055829); a Donaghue Investigator Award; the Betsy and Jonathan Blattmachr family.

References

Aghakhani Y, Bagshaw AP, Benar CG, Hawco C, Andermann F, Dubeau F, et al. fMRI activation during spike and wave discharges in idiopathic generalized epilepsy. Brain 2004; 127: 1127–44.

Andersen AR. 99mTc-D,L-hexamethylene-propyleneamine oxime (99mTc-HMPAO): basic kinetic studies of a tracer of cerebral blood flow. Cerebrovasc Brain Metab Rev 1989; 1: 288–318.

Archer JS, Abbott DF, Waites AB, Jackson GD. fMRI 'deactivation' of the posterior cingulate during generalized spike and wave. Neuroimage 2003; 20: 1915–22.

Avoli M, Gloor P, Kostopoulos G, Naquet T, editors. Generalized epilepsy. Boston: Birkhauser; 1990.

Bell WL, Walczak TS, Shin C, Radtke RA. Painful generalised clonic and tonic–clonic seizures with retained consciousness. J Neurol Neurosurg Psych 1997; 63: 792–5.

Berman R, Negishi M, Spann M, Chung M, Bai X, Purcaro M, et al. Simultaneous EEG, fMRI, and behavioral testing in typical childhood absence seizures. (Submitted for publication).

Blumenfeld H. The thalamus and seizures. Arch Neurol 2002; 59: 135–7.

Blumenfeld H. Cellular and network mechanisms of spike-wave seizures. Epilepsia 2005a; 46 (Suppl 9): 21–33.

Blumenfeld H. Consciousness and epilepsy: why are patients with absence seizures absent? Prog Brain Res 2005b; 150: 271–86.

Blumenfeld H. Epilepsy and consciousness. In: Laureys S, Tononi G, editors. The neurology of consciousness: cognitive neuroscience and neuropathology. Elsevier; 2009.

Blumenfeld H, McNally KA, Ostroff RB, Zubal IG. Targeted prefrontal cortical activation with bifrontal ECT. Psychiatry Res 2003a; 123: 165–70.

Blumenfeld H, McNally KA, Vanderhill SD, Paige AL, Chung R, Davis K, et al. Positive and negative network correlations in temporal lobe epilepsy. Cerebral Cortex 2004a; 14: 892–902.

Blumenfeld H, Rivera M, McNally KA, Davis K, Spencer DD, Spencer SS. Ictal neocortical slowing in temporal lobe epilepsy. Neurology 2004b; 63: 1015–21.

Blumenfeld H, Taylor J. Why do seizures cause loss of consciousness? The Neuroscientist 2003; 9: 301–10.

Blumenfeld H, Westerveld M, Ostroff RB, Vanderhill SD, Freeman J, Necochea A, et al. Selective frontal, parietal and temporal networks in generalized seizures. Neuroimage 2003b; 19: 1556–66.

Brett M, Penny WD, Kiebel SJ. Introduction to random field theory. In: Frackowiak RSJ, Friston KJ, Frith C, Dolan R, Friston KJ, Price CJ, et al., editors. Human brain function. 2nd edn., Ch. 14. Academic Press; 2003.

Brevard ME, Kulkarni P, King JA, Ferris CF. Imaging the neural substrates involved in the genesis of pentylenetetrazol-induced seizures. Epilepsia 2006; 47: 745–54.

Browning RA, Nelson DK. Modification of electroshock and pentylenetetrazol seizure patterns in rats after precollicular transections. Exp Neurol 1986; 93: 546–56.

Chang DJ, Zubal IG, Gottschalk C, Necochea A, Stokking R, Studholme C, et al. Comparison of statistical parametric mapping and SPECT difference imaging in patients with temporal lobe epilepsy. Epilepsia 2002; 43: 68–74.

Cooper IS. Effect of chronic stimulation of anterior cerebellum on neurological disease. Lancet 1973; 1: 206.

Cooper IS, Riklan M, Amin I, Cullinan T. A long-term follow-up study of cerebellar stimulation for the control of epilepsy. In: Cooper IS, editor. Cerebellar stimulation in man. New York: Raven Press; 1978. pp. 19–23.

Dang-Vu TT, Desseilles M, Laureys S, Degueldre C, Perrin F, Phillips C, et al. Cerebral correlates of delta waves during non-REM sleep revisited. Neuroimage 2005; 28: 14–21.

Davidson DL, Barbeau A. Locomotor activity and seizures induced by picrotoxin in the fastigeal nucleus of the rat. Exp Neurol 1975; 49: 622–7.

de Boer HM, Mula M, Sander JW. The global burden and stigma of epilepsy. Epilep Behav 2008; 12: 540–6.

Devous MD Sr, Leroy RF, Homan RW. Single photon emission computed tomography in epilepsy. Seminar Nucl Med 1990; 20: 325–41.

Drazkowski J. An overview of epilepsy and driving. Epilepsia 2007; 48 (Suppl 9): 10–2.

Enev M, McNally KA, Varghese G, Zubal IG, Ostroff RB, Blumenfeld H. Imaging onset and propagation of ECT-induced seizures. Epilepsia 2007; 48: 238–44.

Engel J Jr, Kuhl DE, Phelps ME. Patterns of human local cerebral glucose metabolism during epileptic seizures. Science 1982; 218: 64–6.

Englot DJ, Mishra AM, Mansuripur PK, Herman P, Hyder F, Blumenfeld H. Remote effects of focal hippocampal seizures on the rat neocortex. J Neurosci 2008; 28: 9066–81.

Faingold CL. Neuronal networks in the genetically epilepsy-prone rat. Adv Neurol 1999; 79: 311–21.

Forsgren L, Bucht G, Eriksson S, Bergmark L. Incidence and clinical characterization of unprovoked seizures in adults: a prospective population-based study. Epilepsia 1996; 37: 224–9.

Fraioli B, Guidetti. . Effects of stereotactic lesions of the dentate nucleus of the cerebellum in man. Appl Neurophysiol 1975; 38: 81–90.

Friston KJ, Holmes A, Poline JB, Price CJ, Frith CD. Detecting activations in PET and fMRI: levels of inference and power. Neuroimage 1996; 4: 223–35.

Friston KJ, Worsley KJ, Frackowiak RSJ, Mazziotta JC, Evans AC. Assessing the significance of focal activations using their spatial extent. Hum Brain Map 1994; 2: 210–20.

Gale K. Subcortical structures and pathways involved in convulsive seizure generation. J Clin Neurophysiol 1992; 9: 264–77.

Gotman J, Grova C, Bagshaw A, Kobayashi E, Aghakhani Y, Dubeau F. Generalized epileptic discharges show thalamocortical activation and suspension of the default state of the brain. Proc Natl Acad Sci USA 2005; 102: 15236–40.

Greicius MD, Krasnow B, Reiss AL, Menon V. Functional connectivity in the resting brain: a network analysis of the default mode hypothesis. Proc Natl Acad Sci USA 2003; 100: 253–8.

Hamandi K, Laufs H, Nöth U, Carmichael DW, Duncan JS, Lemieux L. BOLD and perfusion changes during epileptic generalised spike wave activity. NeuroImage 2008; 39: 608–18.

Handforth A, Ackermann RF. Mapping of limbic seizure progressions utilizing the electrogenic status epilepticus model and the ^{14}C-2-deoxyglucose method. Brain Res Brain Res Rev 1995; 20: 1–23.

Handforth A, Treiman DM. Functional mapping of the late stages of status epilepticus in the lithium-pilocarpine model in rat: a ^{14}C-2-deoxyglucose study. Neuroscience 1995; 64: 1075–89.

Holmes MD, Brown M, Tucker DM. Are 'generalized' seizures truly generalized? Evidence of localized mesial frontal and frontopolar discharges in absence. Epilepsia 2004; 45: 1568–79.

Jasper HH. Current evaluation of the concepts of centrencephalic and cortico-reticular seizures. Electroencephalogr Clin Neurophysiol 1991; 78: 2–11.

Jehi L, Najm IM. Sudden unexpected death in epilepsy: impact, mechanisms, and prevention. Cleveland Clin J Med 2008; 75 (Suppl 2): S66–70.

Jobst BC, Williamson PD, Neuschwander TB, Darcey TM, Thadani VM, Roberts DW. Secondarily generalized seizures in mesial temporal epilepsy: clinical characteristics, lateralizing signs, and association with sleep-wake cycle. Epilepsia 2001; 42: 1279–87.

Kotagal P, Luders H, Morris HH, Dinner DS, Wyllie E, Godoy J, et al. Dystonic posturing in complex partial seizures of temporal lobe onset: a new lateralizing sign. Neurology 1989; 39: 196–201.

Kreindler A, Zuckermann E, Steriade M, et al. Electroclinical features of convulsions induced by stimulation of brain stem. J Neurophysiol 1958; 21: 430–6.

Laufs H, Lengler U, Hamandi K, Kleinschmidt A, Krakow K. Linking generalized spike-and-wave discharges and resting state brain activity by using EEG/fMRI in a patient with absence seizures. Epilepsia 2006; 47: 444–8.

McCown TJ, Duncan GE, Johnson KB, Breese GR. Metabolic and functional mapping of the neural network subserving inferior collicular seizure generalization. Brain Res 1995; 701: 117–28.

McNally KA, Paige AL, Varghese G, Zhang H, Novotny EJ, Spencer SS, et al. Localizing value of ictal–interictal SPECT analyzed by SPM (ISAS). Epilepsia 2005; 46: 1450–64.

McNamara JO, Galloway MT, Rigsbee LC, Shin C. Evidence implicating substantia nigra in regulation of kindled seizure threshold. J Neurosci 1984; 4: 2410–7.

Meeren H, van Luijtelaar G, Lopes da Silva F, Coenen A. Evolving concepts on the pathophysiology of absence seizures: the cortical focus theory. Arch Neurol 2005; 62: 371–6.

Meeren HK, Pijn JP, Van Luijtelaar EL, Coenen AM, Lopes da Silva FH. Cortical focus drives widespread corticothalamic networks during spontaneous absence seizures in rats. J Neurosci 2002; 22: 1480–95.

Miller JW. The role of mesencephalic and thalamic arousal systems in experimental seizures. Progr Neurobiol 1992; 39: 155–78.

Moeller F, Siebner HR, Wolff S, Muhle H, Granert O, Jansen O, et al. Simultaneous EEG-fMRI in drug-naive children with newly diagnosed absence epilepsy. Epilepsia 2008 [Epub ahead of print].

Nei M, Bagla R. Seizure-related injury and death. Curr Neurol Neurosci Rep 2007; 7: 335–41.

Nersesyan H, Hyder F, Rothman D, Blumenfeld H. Dynamic fMRI and EEG recordings during spike-wave seizures and generalized tonic–clonic seizures in WAG/Rij rats. J Cereb Blood Flow Metab 2004; 24: 589–99.

Newton MR, Berkovic SF, Austin MC, Reutens DC, McKay WJ, Bladin PF. Dystonia, clinical lateralization, and regional blood flow changes in temporal lobe seizures. Neurology 1992; 42: 371–7.

Norden AD, Blumenfeld H. The role of subcortical structures in human epilepsy. Epilepsy Behav 2002; 3: 219–31.

Parmeggiani A, Posar A, Scaduto MC. Cerebellar hypoplasia, continuous spike-waves during sleep, and neuropsychological and behavioral disorders. J Child Neurol 2008; 23: 1472–6.

Raichle ME, MacLeod AM, Snyder AZ, Powers WJ, Gusnard DA, Shulman GL. A default mode of brain function. Proc Natl Acad Sci USA 2001; 98: 676–82.

Raines A, Anderson RJ. Effects of acute cerebellectomy on maximal electroshock seizures and anticonvulsant efficacy of diazepam in the rat. Epilepsia 1976; 17: 177–82.

Salgado-Benitez A, Briones R, Fernandez-Guardiola A. Purkinje cell responses to a cerebral penicillin-induced epileptogenic focus in the cat. Epilepsia 1982; 23: 597–606.

Schindler K, Leung H, Lehnertz K, Elger CE. How generalised are secondarily 'generalised' tonic clonic seizures? J Neurol Neurosurg Psychiatry 2007; 78: 993–6.

Schridde U, Khubchandani M, Motelow J, Sanganahalli BG, Hyder F, Blumenfeld H. Negative BOLD with large increases in neuronal activity. Cereb Cortex 2008; 18: 1814–27.

Takano H, Motohashi N, Uema T, Ogawa K, Ohnishi T, Nishikawa M, et al. Changes in regional cerebral blood flow during acute electroconvulsive therapy in patients with depression: positron emission tomographic study. Br J Psychiatry 2007; 190: 63–8.

Theodore WH, Porter RJ, Albert P, Kelley K, Bromfield E, Devinsky O, et al. The secondarily generalized tonic–clonic seizure: a videotape analysis. Neurology 1994; 44: 1403–7.

Varghese G, Purcaro MJ, Motelow JE, Enev M, McNally KA, Levin AR, et al. Clinical use of ictal SPECT in secondarily generalized tonic–clonic seizures. Brain 2009, in press.

Wright GDS, McLellan DL, Brice JG. A double-blind trial of chronic cerebellar stimulation in twelve patients with severe epilepsy. J Neurol Neurosurg Psychiatry 1984; 47: 769–74.

Zubal IG, Spencer SS, Imam K, Seibyl J, Smith EO, Wisniewski G, et al. Difference images calculated from ictal and interictal technetium-99m-HMPAO SPECT scans of epilepsy. J Nucl Med 1995; 36: 684–9.